Advances in Nanochemistry

Article

Magnetic functionalized graphene: An efficient and solid acid catalyst for the synthesis of highly functionalized pyrroles under ultrasound irradiation

Received 15th November 2019,
Accepted 30th December 2019,
DOI:10.22126/anc.2019.4787.1017

Sodeh Sadjadi *

Radiation Application Research School, Nuclear Science and Technology Research Institute, Tehran, Iran, P. O. Box: 14399-51113.

Abstract

A simple and efficient ultrasonic-assisted synthesis of highly functionalized pyrroles by a one-pot multi-component strategy using aromatic amines, phenacyl bromide, and dialkyl acetylenedicarboxylate is reported. The reactions were performed in the presence of magnetic functionalized reduced graphene oxide as the catalyst and under environmentally-friendly solventless conditions. Magnetic functionalized graphene was prepared by a three-step processes, 1) functionalization of graphene oxide with diethyl malonate, 2) simultaneous reduction and further functionalization of graphene oxide with hydroxylamine hydrochloride, and 3) synthesis of functionalized graphene/Fe_3O_4 catalyst. High yields, mild reaction conditions, easy work-up, short reaction times, and the reusability of the catalyst are the important features of this protocol.

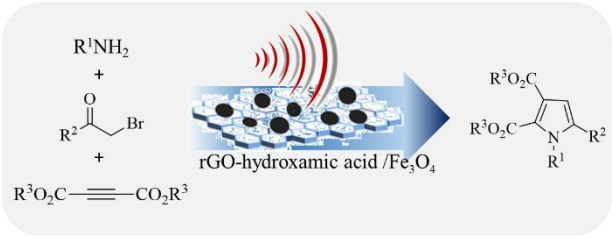

Keywords: *Highly functionalized pyrroles, Ultrasound irradiation, Magnetic functionalized graphene.*

Introduction

Pyrroles are structural motifs that are found in a wide variety of natural products or pharmacologically active substances.[1] Several methods have been developed for the synthesis of pyrrols,[2-4] including the classical Hantzch procedure,[5] Knorr reaction,[6] Paal–Knorr condensation reaction,[7] and various cycloaddition and transition-metal-catalyzed cyclization protocols.[8-11] Despite numerous approaches for the synthesis of pyrroles have been developed, the efficient synthesis of highly functionalized pyrroles remains an attractive goal.

Graphene, the amazing two-dimensional carbon nanomaterial, has drawn immense attention as heterogeneous catalysts in the field of material science due to its very high theoretical surface area, very good mechanical strength, and its amazing electronic properties and thermal conductivity.[12] Graphene-based catalysis is an ongoing research area, which opens new opportunities for graphene applications.[13,14] Graphene oxide consists of oxidized graphene sheets decorated with a large number of oxygen functional groups. The presence of these groups can be served as anchoring sites for other nanomaterials and provides a unique capacity for introducing various functional groups on the surface of graphene. However, the application of graphene as a catalyst is limited by difficult separation and low recovery of the catalyst. This issue can be addressed by the development of the magnetic graphene nanocomposites owing to easy separation by applying a magnetic field.

The use of ultrasound in chemistry offers the synthetic chemists an inexpensive method of chemical activation. The driving force for sonochemistry is cavitation which is the formation, growth, and implosive collapse of bubbles irradiated with sound. This phenomenon creates huge amounts of energy from the conversion of the kinetic energy of the liquid motion into heating the contents of the bubble.[15] When compared with traditional methods, ultrasonic-assisted organic reactions can be conducted in more satisfactory yields, milder reaction conditions, and shorter reaction time.

Combining the advantages of ultrasonic irradiation and nanotechnology, a new method for synthesis of highly functionalized pyrroles using magnetic functionalized graphene was designed under ultrasonic irradiation (Scheme 1).

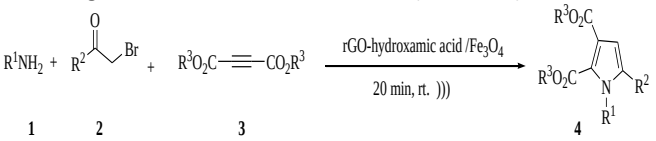

Scheme1. *Catalytic synthesis of highly functionalized pyrroles under ultrasonic irradiation.*

Experimental

Chemicals and instruments

All the chemicals were provided by Merck Company and used

Corresponding author:
Sodeh Sadjadi, Email: sadjadi.s.s@gmail.com

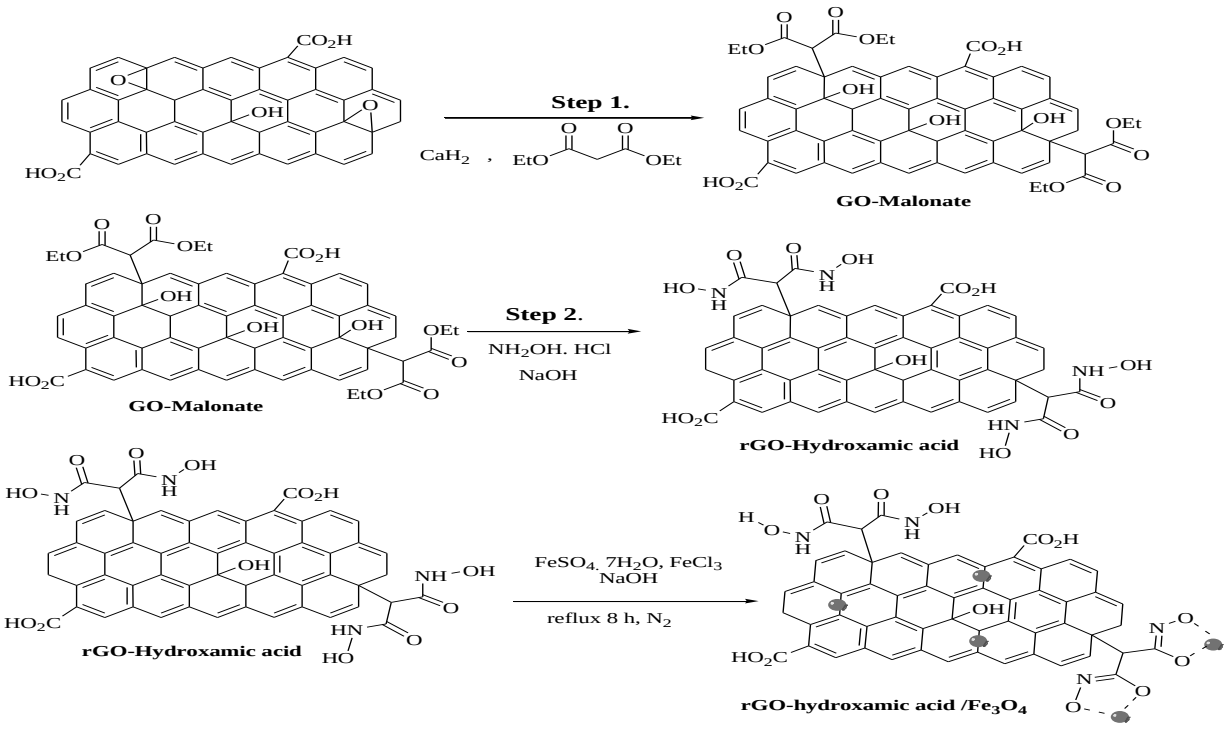

Scheme 2. *The process of preparation of rGO-hydroxamic acid/Fe_3O_4 catalyst.*

without further purification. The FTIR spectra were recorded with a Bruker Vector 22 spectrometer using KBr disks. Melting points were determined using a Barnstead Electrothermal melting point apparatus. The Raman spectra were recorded using Bruker Senterra (Germany) using a 785 nm laser. The scanning electron microscopy (SEM) images elemental maps were recorded by a ZEISS EVO 18 analytic microscope (Germany) equipped with an energy dispersive X-ray (EDS) analyzer. The X-ray diffraction (XRD) pattern of the catalyst was recorded at ambient temperature using a Philips PW 1800 diffractometer. ^{1}H and ^{13}C NMR spectra were recorded at 500 MHz on a Bruker DRX500 spectrometer. The magnetic property of the catalyst was determined by a vibrating sample magnetometer (VSM, Meghnatis Daghigh Kavir Co., Iran). The ultrasound apparatus was a Wiseclear 770W (Seoul, Korea). The operating frequency was 40 kHz and the output power was 200 W.

Catalyst preparation

Preparation of graphene oxide (GO)

Graphene oxide was prepared using a modified Hummers' method.[16] In brief, 13 mL H_3PO_4, and 120 mL H_2SO_4 were added to 1.0 g of graphite powder and mixed by constant stirring at less than 5 °C. Afterward, 6 g of $KMnO_4$ was slowly added under constant and vigorous stirring. When the color of the solution turned to deep brown, the reaction mixture was cooled in an ice bath, diluted to 350 mL and stirred for 30 min. The reaction was quenched with water and hydrogen peroxide (2 mL of H_2O_2 30%). The water reacts with $KMnO_4$ to form MnO_2, effectively stopping the oxidation reaction. The hydrogen peroxide then reacts with MnO_2, reducing it to manganese ions. The product was washed three times with HCl solution (5% wt.) and five times with water and then dried at 60 °C for 14 h.

Preparation of magnetic functionalized graphene (rGO-hydroxamic acid/Fe_3O_4)

The three-step process to fabricate the magnetic functionalized graphene was illustrated in Scheme 2. First, 70 mg CaH_2 was added to 20 mL tetrahydrofuran (THF) and the mixture was cooled to 5 °C. Then, 20 mL of diethyl malonate was added under vigorously stirring conditions (solution A). 0.04 g GO was ultrasonically dispersed in 30 mL THF for 30 min (solution B). Solution A was gradually added to solution B, and the reaction mixture was heated at 60 °C for 24 h. After that, the solid product (GO-malonate) was centrifugally filtered, rinsed with HCl (5% wt) and washed three times with ethanol and then dried at 60 °C for 12 h. In the second step, the reduction of GO and the transformation of ester functional groups into hydroxamic acid were carried out with hydroxylamine hydrochloride. 0.01 g of GO-malonate was dispersed in 40 mL of water, subsequently, 0.02 g of hydroxylamine hydrochloride and 350 µL of sodium hydroxide solution (1.5 M) were added and the mixture was allowed to proceed at 100 °C for 3 h. After the reaction mixture was cooled down to room temperature, the obtained product (rGO-hydroxamic acid) was centrifugally filtered, washed several times with deionized water and ethanol, and dried at 50 °C for 12 h.

Finally, 80 mg of rGO-hydroxamic acid in 30 mL of 0.01 M HCl was ultrasonicated for 30 min, and then a mixture of $FeSO_4.7H_2O$, $FeCl_3$, and NaOH with a molar ratio of Fe^{2+}:Fe^{3+}:OH^- at 1:2:8 was added to this solution. The reaction mixture was refluxed for 8 h under N_2 atmosphere. After cooling, the resulting magnetic functionalized graphene was simply separated by applying a magnetic field and washed with ethanol for 2 times and with water for 4 times.

General procedure for the synthesis of highly functionalized pyrroles

A mixture of aromatic amine **1** (1 mmol), phenacyl bromide **2** (1 mmol), dialkyl acetylenedicarboxylate **3** (1 mmol), and rGO-hydroxamic acid/Fe_3O_4 (0.03 g) was irradiated in the water bath of an ultrasound apparatus at room temperature for 20 min. After completion of the reaction, ethyl acetate (10 mL) was added and the catalyst was removed by applying a magnetic field. Evaporation of the solvent under the reduced pressure followed by purification of the obtained product by column chromatography on silica gel (eluted with 1:7 ethyl acetate/petroleum ether) afforded the pure

product. All products were known and spectral data of the products were the same as those reported in a previously published paper.[17]

Results and discussion

Characterization of catalyst

The powder X-ray diffraction pattern of rGO-hydroxamic acid/Fe_3O_4 catalyst can be found in Figure S1. The diffraction peaks were well matched with JCPDS card No. 65-3107 that confirms the presence of the pure and face- centered cubic spinel structure of magnetite nanoparticles. Moreover, the XRD pattern possesses a characteristic broad diffraction peak at 2θ = 25.1°, which can be indexed as the 002 diffraction peak of reduced graphene oxide.[18]

The FTIR analysis (Figure S2) was performed to confirm 1) the reduction of GO and the presence of the hydroxamic acid groups on its surface, and 2) complex formation between iron and OH of hydroxamic acid group, as proposed in Scheme 2. RGO-hydroxamic acid/Fe_3O_4 spectrum did not show any characteristic peak for the C=O functional group, suggesting that GO was reduced along with functionalization. The characteristic peaks of remaining oxygen-containing functional groups can be seen at 1034, 1208, 1347, 3400, and 1622 cm^{-1} for C-O stretching vibrations in alkoxy and epoxyl groups, C-O-H deformation vibration, hydroxyl groups, and C=C bands, respectively. The band at around 562 cm^{-1} was assigned to the F-O bonds (Fe-N band does not have adsorption in mid-IR) which confirmed the chemical attachment of Fe_3O_4 nanoparticles to the functionalized graphene. A band at 1631 cm^{-1} can be attributed to the C=O stretching of -CONHOH group. The other peak at 1205 cm^{-1} corresponds to C–N stretching absorption.[19,20]

The surface morphology and elemental composition of rGO-hydroxamic acid/Fe_3O_4 were determined by SEM/EDX. As shown in Figure 1, the rGO-hydroxamic acid displays a flake characteristic of graphene with wrinkled texture and the synthesized Fe_3O_4 nanoparticles show well-defined spherical shapes. This observation was further confirmed by EDX analysis (Figure 1B and Table S1) and elemental mapping (Figure 1C), where C, O, N, and Fe were found in the structure of functionalized graphene.

The Raman spectra of the magnetic functionalized rGO nanocomposite compared with the pristine GO are shown in Figure 2. Generally, the spectra show the characteristic G peak at 1578 cm^{-1}, which is due to the graphitic domain of E2g symmetry, and the D band at 1335 cm^{-1}, which stems from structural defects and A1g symmetry. The Raman spectrum of the magnetic functionalized rGO nanocomposite exhibits an increase in the intensity of the D band relative to the G band (from I_D/I_G = 1.7 for GO to I_D/I_G = 1.002 for rGO-hydroxamic acid/Fe_3O_4), suggesting more structural defects induced during the introduction of Fe_3O_4 nanoparticles, the functionalization process and the formation of sp^3 hybridized carbon due to covalent attachment of diethyl malonate. Moreover, G band for rGO-hydroxamic acid/Fe_3O_4 downshifted by 5 cm^{-1} comparing to that for GO, due to the efficient charge transfer between rGO and Fe_3O_4, indicating a strong interaction between rGO-hydroxamic acid and Fe_3O_4 nanoparticles.[21]

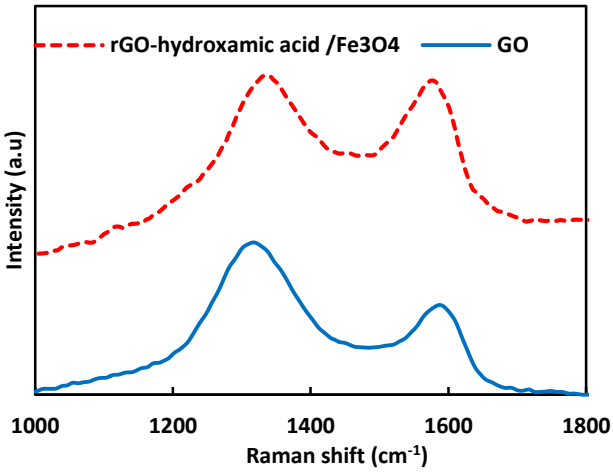

Figure 2. *The Raman spectra of GO and rGO-hydroxamic acid/Fe_3O_4.*

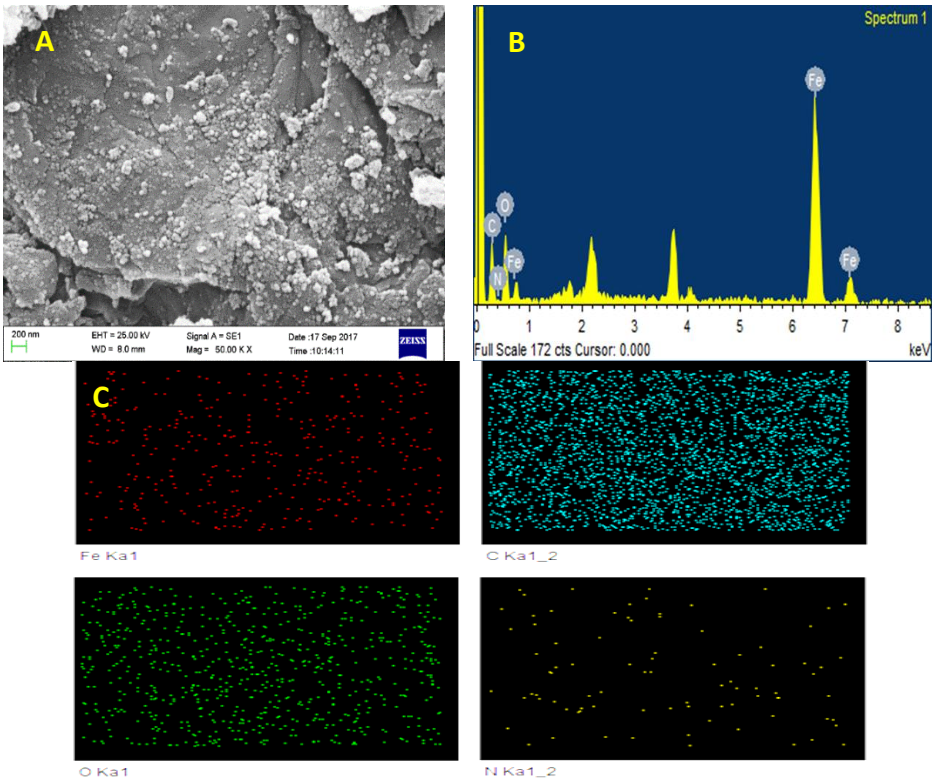

Figure 1. *The (A) SEM image, (B) EDX analysis spectra, and (C) elemental maps of rGO-hydroxamic acid/Fe_3O_4 catalyst*

Table 1. *The reaction of aniline, α-bromo acetophenone, and dimethyl acetylenedicarboxylate under different reaction conditions.*

Entry	Conditions	Catalyst	Time (min)	Yield (%)
1	Stirring / rt	rGO-hydroxamic acid/Fe_3O_4 (0.03 g)	75	81
2	Stirring / rt	Without catalyst	60	No product
3	Ultrasound-assisted / rt	Without catalyst	20	15
4	Ultrasound-assisted / rt	Without catalyst	60	15
5	Ultrasound-assisted / rt	rGO-hydroxamic acid/Fe_3O_4 (0.01 g)	20	74
6	Ultrasound-assisted / rt	rGO-hydroxamic acid/Fe_3O_4 (0.03 g)	20	97
7	Ultrasound-assisted /rt	rGO-hydroxamic acid/Fe_3O_4 (0.05 g)	20	97

The magnetic property of the synthesized rGO-hydroxamic acid/Fe_3O_4 was also investigated by VSM analysis (Figure 3). The magnetic hysteresis curve showed that synthesized rGO-hydroxamic acid/Fe_3O_4 is essentially superparamagnetic. RGO-hydroxamic acid/Fe_3O_4 and Fe_3O_4 have a magnetization saturation value of 60.5 and 72.2 emu g^{-1}, respectively.

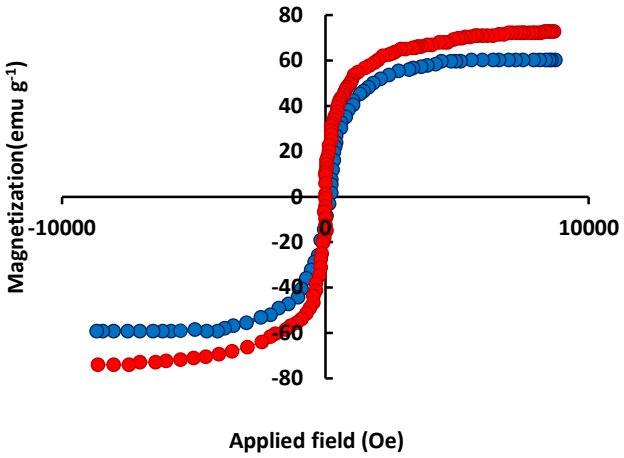

Figure 3. *The VSM spectrum of rGO-hydroxamic acid/Fe_3O_4 (blue curve) and Fe_3O_4 nanoparticles (red curve).*

Catalytic test

In order to identify suitable reaction conditions and determine the catalytic efficiency of rGO-hydroxamic acid/Fe_3O_4, a three-component reaction between aniline (1 mmol), α-bromo acetophenone (1 mmol), and dimethyl acetylenedicarboxylate (1 mmol) as a model reaction was conducted under different operating conditions (Table 1). The reaction mixture was sonicated for 20 min at room temperature, and the pyrrole **4a** was obtained in 97% yield with the optimum amount of catalyst, 0.03 g (Table 1). Further increase in catalyst dosage to 0.05 g only slightly increased the yield to 97%. Without the catalyst, the same reaction generated only 15% of pyrrole **4a** over the same period of time under ultrasonic irradiation. No improvement in yield was observed even after 1 h.

Further experiment was run under stirring condition to get insights into the role of ultrasonic irradiation (Table 1). It is obvious that under the same reaction conditions, a higher yield can be obtained at shorter reaction time under ultrasonic irradiation.

A plausible reaction mechanism for the synthesis of highly functionalized pyrroles is depicted in Scheme 3. Initially, dialkyl acetylenedicarboxylate **3** is activated with rGO-hydroxamic acid/Fe_3O_4 through the formation of the intermolecular hydrogen-bonded intermediate **A**. Then, Michael-type addition of amine **1** with **A** provides the α,β-unsaturated *N*-arylamine intermediate **B**. Intermediate **B** then reacts with phenacyl bromide **2** to produce intermediate **C**. Finally by dehydration of intermediate **C**, compound **4** is generated.

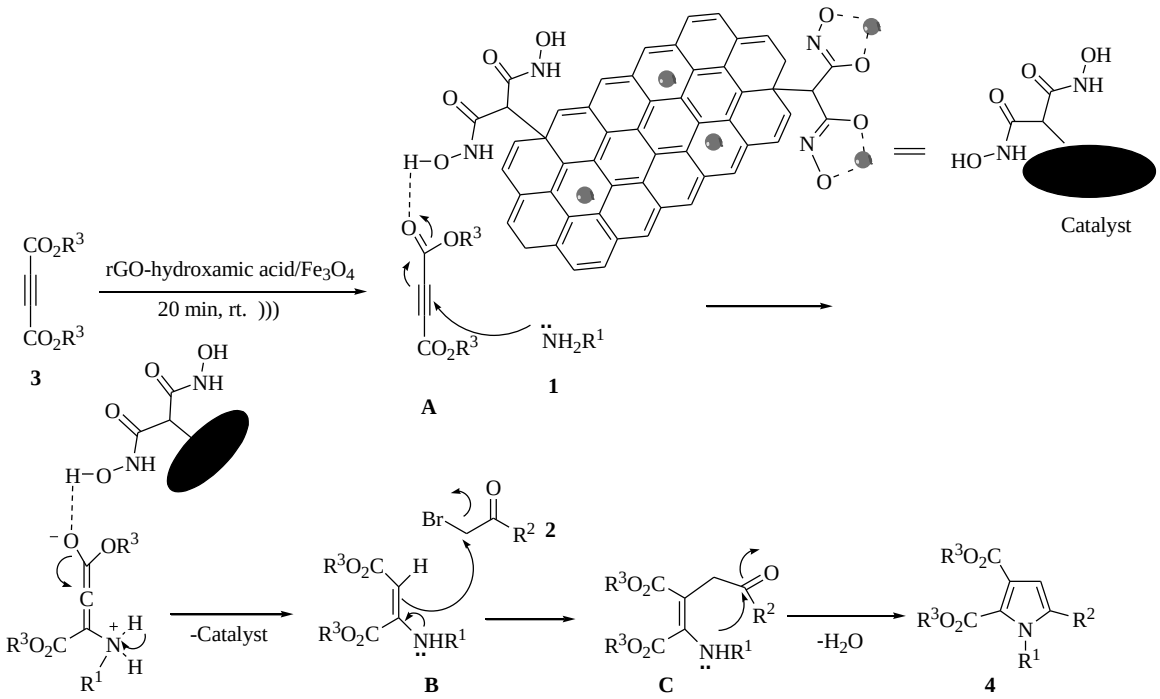

Scheme 3. *A plausible reaction mechanism for the synthesis of highly functionalized pyrroles.*

To establish the generality of this method, the synthesis of various substituted pyrroles was investigated. The reaction of various aromatic amines bearing an electron-donating group with various phenacyl bromide with an electron-withdrawing group and dialkyl acetylenedicarboxylate afforded the corresponding pyrroles in 93‑97% yields (Table 2). When the electron-withdrawing group was attached to the aniline, the lower yield for product **4** was observed, and a notable amount of alkyne substrate **3** was recovered. The yield of product **4** also decreased by using phenacyl bromide **2** bearing a strongly electron-donating group. These results agree well with the proposed mechanism to substituted pyrroles **4** which is based on nucleophilic Michael addition of the primary amine **1** to dialkyl acetylenedicarboxylate **3**, followed by addition of intermediate **B** to an electrophilic α-carbon atom of phenacyl bromide **2** (Scheme 3).

To show the merit of this method, the yield of **4b** in the presence of rGO-hydroxamic acid/Fe_3O_4 under ultrasonic irradiation was compared with previously reported catalysts (Table 3). The results show that the three-component reaction catalyzed by rGO-hydroxamic acid/Fe_3O_4 under ultrasonic irradiation proceeds over shorter reaction time and affords higher product yield.

The reusability of the catalyst was also tested in the model reaction under the optimized conditions to investigate how the catalyst performs in repeated runs. The recovered catalyst was washed with ethyl acetate, dried at 60 °C for 12 h and reused in another run of reaction. The catalyst was found to be reusable for three cycles with only a gradual decrease in its activity. The model reaction afforded the corresponding pyrrole in 96, 93, and 89% yields over three successive runs.

Table 2. *Catalytic synthesis of highly functionalized pyrroles under ultrasonic irradiation. (For Entry 1-5, amine is aniline, for Entry 6 and 7, amine is 4-methyl aniline, for Entry 8, amine is 4-methoxy aniline.)*

Entry	Dialkyl acetylene dicarboxylate	α-Bromo ketone	Product	Yield* (%)
1	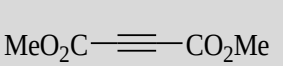	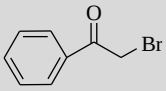	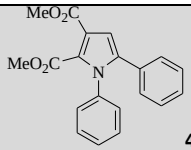 **4a**	97
2	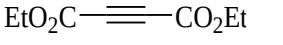	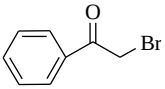	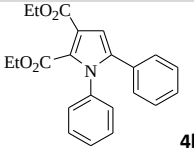 **4b**	94
3	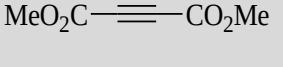	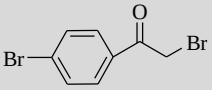	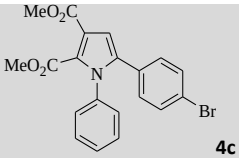 **4c**	95
4		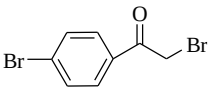	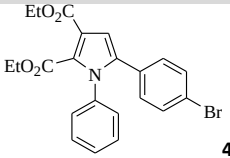 **4d**	92
5		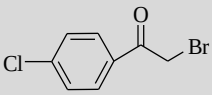	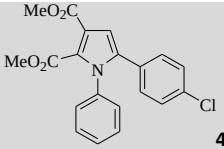 **4e**	93
6		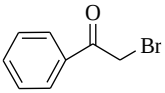	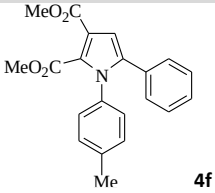 **4f**	97
7		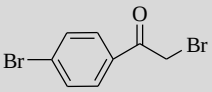	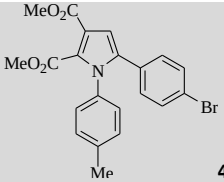 **4g**	95
8		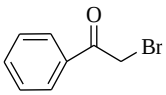	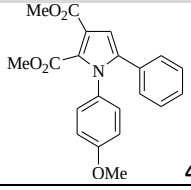 **4h**	97

*Yields refer to isolated products.

Table 3. *Comparison of the reported catalytic methods for the synthesis of highly functionalized pyrrole* ***4b*** *in different conditions.*

Entry	Catalyst	Time	Conditions	Yield (%)	Reference
1	PEG - 400	10 h	Stirring at 60 °C	89	20
2	ionic liquid [bmim]BF_4	60 min	Stirring at rt.	87	21
3	β-cyclodextrin	Not reported	Stirring in water at 60 °C	88	22
4	$FeCl_3$	14 h	Stirring in CH_2Cl_2 at rt.	89	23
5	$ZnCl_2$	14 h	Stirring in CH_2Cl_2 at rt.	45	23
6	$H_3PW_{12}O_{40}$	1 h	Stirring at rt.	92	17
7	rGO-hydroxamic acid/Fe_3O_4	20 min	Stirring at rt. ultrasonic irradiation	94	This work

Conclusion

This research work demonstrates a simple and highly efficient methodology for the synthesis of highly functionalized pyrroles in the presence of rGO-hydroxamic acid/Fe_3O_4 catalyst under ultrasound irradiation. A simple workup procedure, mild reaction conditions, a recyclable catalyst, and good yields make this methodology a valid contribution to the existing processes in the field of pyrrole derivatives.

References

1. F. M. Istrate and F. Gagosz, *Org. Lett.*, 9, **2007**, 3181.
2. M. Gao, W. Zhao, H. Zhao, Z. Lin, D. Zhang, and H. Huang, *Beilstein J. Org. Chem.*, 14, **2018**, 884.
3. Y. -C. Hsu, S.-A. Hsieh, P.-H. Lia, and R.-S. Liu, *Chem. Commun.*, 54, **2018**, 2114.
4. L. Marin, V. Gandon, E. Schulz, and D. Lebœuf, *Adv. Synth. Catal.*, 359, **2017**, 1157.
5. M. S. T. Morin, D. J. St-Cyr, and B. A. Arndtsen, *Org. Lett.*, 12, **2010**, 4916.
6. L. Knorr, *Chem. Ber.*, 17, **1884**, 1635.
7. C. Paal, *Ber. Dtsch. Chem. Ges.*, 18, **1885**, 367.
8. N. K. Pahadi, M. Paley, R. Jana, S. R. Waetzig, and J. A. Tunge, *J. Am. Chem. Soc.*, 131, **2009**, 16626.
9. J. -Y. Wang, X. -P. Wang, Z. -S. Yu, and W. Yu, *Adv. Synth. Catal.*, 351, **2009**, 2063.
10. C. V. Galliford and K. A. Scheidt, *J. Org. Chem.*, 72, **2007**, 1811.
11. O.A. Attanasi, G. Favi, F. Mantellini, G. Moscatelli, and S. Santeusanio, *J. Org. Chem.*, 76, **2011**, 2860.
12. A. Ghosh, S. Basu, and A. Verma, *Fuel Cells*, 13, **2013**, 355.
13. M. Golestanzadeh, H. Naeimi, and Z. Zahraie, *Mat. Sci. Eng.*, 71, **2017**, 709.
14. S. Sadjadi, *Iran. J. Catal.*, 8, **2018**, 189.
15. R. Patil, P. Bhoir, P. Deshpande, T. Wattamwar, M. Shirude, and P. Chaskar, *Ultrason. Sonochem.*, 6, **2013**,1327.
16. L. Irannejad, S. J. Ahmadi, S. Sadjadi, and M. Shamsipur, *J. Iran Chem. Soc.*, 15, **2018**, 111.
17. M. Soltani, I. Mohammadpoor-Balto, A. R. Khosropour, M. Moghadam, S. Tangestaninejad, and V. Mirkhani, *C. R. Chim.*, 19, **2016**, 381.
18. A. Jafaryan, S. Sadjadi, A. Gharib, and S. J. Ahmadi, *Appl. Organomet. Chem.*, 33, **2019**, 5085.
19. M. M. Mezgebe, Z. Yan, G. Wei, S. Gong, F. Zhang, S. Guang, and H. Xu, *Mater. Today*, 5, **2017**, 164.
20. L. Nagarapu, R. Mallepalli, L. Yeramanchi, and R. Bantu, *Tetrahedron Lett.*, 52, **2011**, 3401.
21. I. R. Siddiqui, D. Kumar, and S. Shamim, *J. Heterocycl. Chem.*, 50, **2013**, E111.
22. K. Ramesh, K. Karnakar, G. Satish, and Y.V.D. Nageswar, *Chin. Chem. Lett.*, 23, **2012**, 1331.
23. B. Das, G. C. Reddy, P. Balasubramanyam, and B. Veeranjaneyulu, *Synthesis*, 10, **2010**, 1625.